Published online 8 February 2013 *Nucleic Acids Research, 2013, Vol. 41, No. 6* ***3673–3687***
doi:10.1093/nar/gkt066

The small molecule Retro-1 enhances the pharmacological actions of antisense and splice switching oligonucleotides

Xin Ming[1], Kyle Carver[1], Michael Fisher[1], Romain Noel[2], Jean-Christophe Cintrat[2], Daniel Gillet[3], Julien Barbier[3], Canhong Cao[1], John Bauman[1] and Rudolph L. Juliano[1,*]

[1]Division of Molecular Pharmaceutics, UNC Eshelman School of Pharmacy, University of North Carolina, Chapel Hill, NC 27599, USA, [2]CEA, DSV, iBiTec-S, SCBM, 91191 Gif sur Yvette, France and [3]CEA, DSV, iBiTec-S, SIMOPRO, 91191 Gif sur Yvette, France

Received June 25, 2012; Revised January 14, 2013; Accepted January 17, 2013

ABSTRACT

The attainment of strong pharmacological effects with oligonucleotides is hampered by inefficient access of these molecules to their sites of action in the cytosol or nucleus. Attempts to address this problem with lipid or polymeric delivery systems have been only partially successful. Here, we describe a novel alternative approach involving the use of a non-toxic small molecule to enhance the pharmacological effects of oligonucleotides. The compound Retro-1 was discovered in a screen for small molecules that reduce the actions of bacterial toxins and has been shown to block the retrograde trafficking pathway. We demonstrate that Retro-1 can also substantially enhance the effectiveness of antisense and splice switching oligonucleotides in cell culture. This effect occurs at the level of intracellular trafficking or processing and is correlated with increased oligonucleotide accumulation in the nucleus but does not involve the perturbation of lysosomal compartments. We also show that Retro-1 can alter the effectiveness of splice switching oligonucleotides in the *in vivo* setting. These observations indicate that it is possible to enhance the pharmacological actions of oligonucleotides using non-toxic and non-lysosomotropic small molecule adjuncts.

INTRODUCTION

The manipulation of gene expression through use of chemically synthesized oligonucleotides has had a dramatic impact on basic biomedical research and also offers the promise of powerful new approaches for treatment of human disease. Currently, four broad categories of oligonucleotides have evinced significant therapeutic potential including siRNA, miRNA, 'classic' antisense oligonucleotides (ASOs) and splice-switching oligonucleotides (SSOs). Interference by double-stranded RNA is a key endogenous mechanism of gene regulation involving mRNA degradation and/or sequestration, translation arrest and effects on chromatin (1,2). Although siRNA-'slicing' activity mediated by the Ago2/RISC complex in the cytosol requires full complementarity, short dsRNAs can also display miRNA activity against partially complementary sequences, leading to translation arrest, sequestration in P-bodies and degradation. The primary mode of action of 'classic' single strand ASOs is RNase H-mediated degradation of complementary pre-mRNA in the nucleus (3). However, chemically modified ASOs that do not support RNase H activity can alter nuclear pre-mRNA splicing by blocking interactions with splicesosomes, thus acting as SSOs (4).

There are multiple ongoing clinical trials involving various types of oligonucleotides including siRNA, ASOs and SSOs, testifying to the immense interest in this broad therapeutic approach (3–8). Nonetheless, oligonucleotide-based therapies face a key problem

*To whom correspondence should be addressed. Tel: +1 919 966 4383; Fax: +1 919 966 5640; Email: arjay@med.unc.edu
Correspondence may also be addressed to Daniel Gillet. Tel: +33 1 69 08 76 46; Fax: +33 6 88 21 08 73; Email: daniel.gillet@cea.fr

The authors wish it to be known that, in their opinion, the first two authors should be regarded as joint First Authors.

regarding the inefficient access of these large, highly polar molecules to their sites of action in the nucleus or cytosol of tissue cells (9,10). Chemical modification of oligonucleotides to improve stability and efficacy (8,11) as well as the use of various nanotechnology-based delivery approaches (12–17) have been very helpful in this regard. Other important delivery approaches include the chemical conjugation or complexation of oligonucleotides with cell-penetrating peptides designed to promote endsomal escape (18–20), as well as conjugation of oligonucleotides with ligands intended to promote receptor-selective cell uptake (21–24). Despite these various approaches, however, the access problem remains challenging. For example, restricted biodistribution (10), as well as toxicities ascribed to cationic constituents (25), have been problematic for the use of lipid or polymer nanoparticles in oligonucleotide therapeutics. Therefore, it is clear that the discovery of alternative strategies to enhance the access of oligonucleotides to their intracellular targets will have substantial value for oligonucleotide-based pharmacology and therapeutics.

Oligonucleotides are usually internalized via endocytosis and then traffic through various membrane-circumscribed vesicular compartments (9,26,27). Cells use multiple distinct endocytotic uptake mechanisms including the clathrin pit pathway, the caveolar pathway, one or more caveolin and clathrin-independent pathways and macropinocytosis. Initial uptake is followed by trafficking into a variety of endomembrane compartments including early/sorting endosomes, late endosomes/multi-vesicular bodies, lysosomes and the *trans*-Golgi network (TGN) (28,29). Most of the oligonucleotide accumulated in cells remains sequestered in various endomembrane vesicles and is pharmacologically inert, but a small fraction escapes to the cytosol and nucleus to permit activity (26,30). Recently, there has been substantial interest in understanding the intracellular trafficking of oligonucleotides and their delivery modalities (31–34). In particular we, and others, have found that the pathway of uptake and intracellular trafficking can have a strong effect on the pharmacological activity of an oligonucleotide; there are productive and less-productive pathways (35–39). These observations suggest that if it was possible to influence the intracellular trafficking of oligonucleotides, and their release from endomembrane compartments, one might be able to substantially enhance their pharmacological effects.

Although molecular biological tools for manipulating vesicular trafficking exist (40), there has been a paucity of chemical tools available for this purpose. Recently, however, a group of compounds that profoundly and selectively affect intracellular traffic have been described (41). These molecules, termed 'Retro' compounds, came from a high throughput screen for small molecules that reduce the harmful actions of bacterial and plant toxins. The Retro compounds block the retrograde trafficking pathway (42) used by many toxins by interfering with shuttling between endosomes and the TGN. Although the precise intracellular trafficking pathways used by various types of oligonucleotides are not well defined at this point, we nonetheless decided to test the possibility that the Retro compounds might beneficially influence the intracellular trafficking of oligonucleotides so as to enhance their pharmacological effects.

MATERIALS AND METHODS

Reagents and cells

Splice switching 2′-O-Me phosphorothioate oligonucleotide 623 (5′-GTTATTCTTTAGAATGGTGC-3′), its 5-base mismatch (5′-GTAATTATTTATAATCGT CC-3′), as well as 3′-TAMRA fluorophore-labelled versions were synthesized in our laboratory as described (35) or custom synthesized by Girindus America (Cincinnati, OH). The anti-MDR1 antisense oligonucleotide (5′-CCATCccgacctcgcGCTCC-3′) (43) and its scrambled control were synthesized by Integrated DNA Technologies (Coralville, IA), as were an anti-Bcl-x oligonucleotide (5′-CTACGctttccacgcACAGT-3′) and its mismatched control (5′-CGACAcgtacctctcGCATT-3′) (44). These several oligomers were phosphorothioate gapmers with 2′-O-Me modifications at the capitalized positions. A previously described MDR1 siRNA (45) was prepared by Dharmacon Inc (Lafayette, CO). A SSO (5′-TGGTTCTT ACCCAGCCGCCG-3′) that causes redirection of Bcl-x pre-mRNA splicing from Bcl-xL to –xS has been previously described (46). A fluorescein isothiocyanate-tagged monoclonal antibody to P-glycoprotein (Pgp) was from BD-Pharmingen (San Jose, CA). LysoTracker Green lysosomotropic dye, Lipofectamine 2000 and baculovirus expression systems (*Organelle* Lights^{TM}) were obtained from Invitrogen (Carlsbad, CA, USA). Plasmids coding for green fluorescent protein (GFP) chimeras of Rab 5, Rab 9 and Rab 11 were kindly provided by Prof. Bo van Deurs (University of Copenhagen, Denmark) and Dr. S. Pfeffer (Stanford University, USA). A375Luc705 is a human melanoma cell line containing a firefly luciferase coding sequence interrupted by an abnormal intron (35). HeLaEGFP654 is a human cell line containing an enhanced GFP reporter interrupted by an abnormal intron; HeLaLuc705 contains a similarly structured luciferase reporter (both obtained from R. Kole, AVI Biopharma). In each of these cell lines, correct splicing and reporter expression can be restored by delivery of the 623 SSO to the nucleus. NIH-3T3-MDR is a mouse fibroblast cell line stably transfected with a complementary DNA (cDNA) coding for the human Pgp and was obtained from M. Gottesmann (National Cancer Institute). PC3 human prostate tumour cells were obtained from the UNC Lineberger Cancer Center. Retro-1 was synthesized and characterized as previously described (41). The ClogP value of Retro-1 was calculated using ChemBioDraw Ultra 12.0.

SSO-mediated induction assays

Typically, A375Luc705, HeLa Luc705 or HeLaEGFP654 cells were incubated with SSO 623 or control mismatch oligonucleotide in serum-free OPTI-MEM I for 4 h followed by addition of fetal bovine serum (FBS) to 1.5% for an additional 12 h. The oligonucleotides were removed, and the cells rinsed in buffer; thereafter,

medium plus 1.5% FBS was added followed by various amounts of Retro-1 in dimethylsulfoxide (DMSO). The Retro compound was removed after 2 h, and the cells further incubated in medium plus 1.5% FBS for an additional period. Deviations from this procedure are noted in the figure legends. In some cases, cells were treated with SSO 623 and Lipofectamine 2000 as a positive control. Luciferase enzyme activity was determined as previously described (39). Enhanced green fluorescent protein (EGFP) expression was measured by flow cytometry using an LSR II cell analyser (Becton-Dickenson, San Jose, CA, USA) with a 488-nm laser coupled with a 525/50 filter for EGFP.

Pgp assays

NIH-3T3-MDR cells were incubated with various concentrations of anti-MDR1 or mismatched antisense oligonucleotide in Dulbecco's modified Eagle's medium-H plus 2% FBS for 4 h. The oligonucleotides were removed by rinsing, and medium + 2% FBS was added followed by the addition of Retro-1 at various concentrations. After 4 h, the Retro compound was removed, and incubation continued for 48 h. In some cases, cells were treated with oligonucleotide and Lipofectamine 2000 as a positive control. The same procedure was followed for treatment of cells with MDR1-siRNA. Pgp expression was measured essentially as previously described (47) using fluorescein isothiocyanate-tagged anti-Pgp antibody and flow cytometry. Pgp transport activity in NIH-3T3-MDR cells was measured by cytometry using accumulation of tetramethylrosamine, a fluorescent Pgp substrate (48).

RNA isolation and analysis (Reverse transcriptase-polymerase chain reaction)

Total RNA was isolated using TriReagent (Molecular Research Center, Cincinnati, OH, USA). Total RNA was converted into first-strand cDNA using Enhanced Avian First Strand Synthesis Kit (Sigma). EGFP cDNA was amplified by PCR using forward (5′-CGTAAACGGC CACAAGTTCAGCG-3′) and reverse (5′-GTGGTGCAG ATGAACTTCAGGGTC-3′) primers, whereas Luciferase cDNA was amplified using forward (5′-TTGATATGTG GATTTCGAGTCGTC-3′) and reverse (5′-TGTCAATC AGAGTGCTTTTGGCG-3′) primers. Primers for Bcl-x amplification were 5′-CATGGCAGCAGTAAAGCA AG-3′ and 5′-GCATTGTTCCCATAGAGTCC-3′. Primers for beta-actin amplification were 5′-CTGGGAC GACATGGAGAAAA-3′ and 5′-AAGGAAGGCTGGA AGAGTGC-3′. Cycles of PCR proceeded at 94°C for 30 s, 65°C for 30 s and 72°C for 60 s for 30 cycles. The PCR products were separated on agarose gels, and bands were visualized and quantitated using a Gel Doc imaging system (Bio-Rad, Hercules, CA, USA).

Cytotoxicity

Cells were seeded in 96-well plates at 5000 cells/well. After 24 h, cells were exposed to different concentrations of Retro-1 for 4 h. Drug-containing medium was replaced with fresh medium, and cells were incubated for an additional 24 h. An Alamar Blue assay (49) was used to measure cytotoxicity. A lactate dehyrogenase release assay for plasma membrane integrity was performed using a commercial kit according to manufacturer's specifications (Clontec, Mt View, CA).

Confocal microscopy and co-localization with endomembrane markers

Live cell confocal microscopy was performed to examine the subcellular distribution of fluorescent oligonucleotide or of certain markers for endomembrane compartments. In some cases, cells (HeLa) were transfected with plasmids encoding GFP chimeras of Rab 9 or 11. Alternatively, the cells were transfected with baculovirus expression vectors (Life Technologies, *Organelle* Lights™) for GFP chimeras of Rab 5, Rab 7, lysosome-associated membrane glycoprotein 1 (LAMP-1) or for a Golgi marker. The day following transfection cells were incubated with carboxytetramethylrhodamine (TAMRA) conjugated SSO 623 in OptiMEM media after which the cells were washed and incubated in dulbecco's modified Eagle's medium with 1% serum. Specific times and concentrations are indicated in the figure legends. Cells were imaged on an Olympus FV1000 MPE laser scanning confocal microscope with environmental chamber to maintain 37°C, 40% humidity and 5% CO_2 ; 488 nm (GFP) and 559 nm (TAMRA) were used as laser lines, and images were collected with an 60× oil immersion lens. Alternatively, a Zeiss 510 Meta laser scanning confocal microscope was used. For kinetic studies, images were captured every minute for 5 min before the addition of Retro-1 (100 μM) and for 20 min after. Quantification was performed in FV10-ASW software. Co-localization is represented as the Pearson Coefficient (50) of GFP and TAMRA overlap within the cytoplasm of the cell. Nuclear intensity is the ratio of nuclear and whole cell means of TAMRA fluorescence.

In vivo experiments

Non-obese diabetic (NOD) *scid* mice (Jackson Laboratories) received bilateral sub-cutaneous xenografts of 2×10^6 A375Luc705 human melanoma cells, and tumours were allowed to grow to ~0.5 cm. Thereafter, on successive days, mice received intra-peritoneal injections of 200 μl of buffered saline or of SSO 623 in buffered saline (20 mg/kg 2×, 40 mg/kg 1×). At 18 h after the last injection, the mice were imaged for luciferase activity. Immediately thereafter, a cohort of the mice received a single 40 μl intra-venous injection of 2 mg of Retro-1 using DMSO/PEG400 (50/50) as a diluent. At 6 h after receiving the Retro-1, all animals were imaged again. For quantitation of luciferase induction (51), the mice were injected subcutaneously with luciferin and imaged in a Xenogen IVIS™ system with continuous isoflurane anesthesia; luminescence was measured and analysed using Living Image® software. At the termination of the experiment, the mice were euthanized using AAALAC approved methods, and tumour and blood samples were collected. Tumour samples were analysed for splice correction of luciferase reporter RNA and

luciferase enzyme activity. Blood samples were analysed by the UNC Animal Clinical Chemistry Core facility.

RESULTS

We investigated the effects of the compound Retro-1 on the intracellular processing and pharmacological effectiveness of oligonucleotides primarily by making use of two types of model systems. The first model tests effects of SSOs in cultured cells stably transfected with a cassette comprising the coding sequence of a reporter gene interrupted by an abnormal intron (4,39). Delivery of an appropriate SSO to the cell nucleus results in corrected splicing and increased expression of the reporter. A second type of model tests the ability of classic ASOs or siRNA to reduce the expression of a target. In this case, the principal chosen target is the *MDR1* gene product Pgp (ABCB1), a membrane transporter involved in cancer drug resistance (52). Expression of Pgp in drug-resistant cells is assayed using a monoclonal anti-Pgp antibody and flow cytometry (47). In both models, cells were treated with oligonucleotides in the absence of any transfection agent, the oligonucleotides were rinsed away, and the cells were then briefly treated with the Retro compound. At intervals after removal of the Retro compound, the pharmacological effects of the oligonucleotides were measured. The structure of Retro-1 has been previously described (41) and is depicted in Figure 1. Retro-1 has a calculated log P of 3.33, and thus it should readily pass across cell membranes by diffusion (53).

Retro-1 enhances the actions of SSOs

We found that increasing concentrations of Retro-1 progressively enhanced the actions of a SSO on a luciferase reporter stably transfected into HeLa cells (Figure 2a). For example, at 100 μM Retro-1, there was ~10-fold increase in the luciferase induction produced by 50 nM SSO as compared with when no Retro compound was added. We examined the kinetics of the process by harvesting the cells at various times after removal of Retro-1 and found that the luciferase signal peaked at ~6 h (Figure 2b). Thus, Retro-1 treatment caused a delayed transient increase in luciferase activity.

We also tested the ability of Retro-1 to alter the action of a SSO that targets an EGFP reporter stably transfected into HeLa cells. As seen in Figure 2c, Retro-1 increased the induction of EGFP by the SSO; the effect was not as robust as that produced using a cationic lipid to deliver the oligonucleotide, but nonetheless was substantial. The observations on the induction of EGFP at the protein level were paralleled by correction of splicing of EGFP mRNA (Figure 2d). As seen in Figure 2c, both cells treated with SSO plus Retro-1 and those treated with with SSO plus cationic lipid exhibited heterogeneous responses, with only a fraction of the cells affected; it has been our experience that this is typical for experiments with various oligonucleotides, no matter what delivery agent is used (33,47).

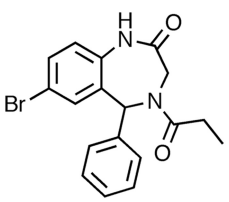

Figure 1. Structure of Retro-1.

Retro-1 can also enhance the effects of SSOs that influence expression of endogenous genes. Thus, an SSO that alters the splicing of Bcl-x pre-mRNA to increase production of the pro-apoptotic Bcl-x_S form showed increased effectiveness in the presence of Retro-1 (Figure 3a and b). The effect was not as robust as that attained with delivery of the SSO using cationic lipid transfection (~14% versus 60% splice switching), but nonetheless was readily observable.

To further explore mechanisms, we used A375Luc705 human melanoma cells and found that the Retro compound increased luciferase induction in the presence of an active SSO but had no effect in the presence of a mismatched control oligonucleotide, indicating that Retro-1 does not cause a non-specific increase in splicing activity (Figure 3c). We then examined the effect of Retro-1 when the SSO was delivered by electroporation, thus bypassing endocytosis and intracellular trafficking, and found no enhancement of the SSO effect by the Retro agent (Figure 3d). Therefore, it seems that Retro-1 acts by altering the intracellular processing of the SSO rather than directly on the splicing machinery.

We also examined the relationship between the kinetics of cellular uptake of the SSO- and Retro-1-induced luciferase expression. As seen in Supplementary Figure S1a, there was gradual accumulation of TAMRA fluorophore-labelled SSO in HeLaLuc705 cells at both low (20 nM) and High (500 nM) concentrations. By using these two very different SSO concentrations, we were able to select points where the cells had accumulated approximately the same amount of oligonucleotide but had been exposed to the oligonucleotide for different periods. As seen in Supplementary Figure S1b, both the total amount of oligonucleotide accumulated and the duration of exposure affected Retro-1-induced luciferase expression, especially at early times of uptake. This suggests that the SSO needs time to move from early compartments, where it accumulates immediately after uptake, to later stage endomembrane compartments that can be affected by Retro-1. Thus, in summary, the set of experiments in Figures 2 and 3 and Supplementary Figure S1 demonstrates that Retro-1 can significantly enhance the actions of SSOs on the expression of reporter genes and endogenous genes in a concentration and time-dependent manner.

Although we did not anticipate that there would be any direct interaction between Retro-1 and oligonucleotides, we sought to rule out this possibility using a spectroscopic assay. Thus, Supplementary Figure S2 shows that there were no changes in the optical spectra of the SSO or the Retro-1 on mixing, indicating a lack of interaction.

Retro-1 enhances the actions of ASOs, but not siRNAs

We also examined the effects of the Retro compound on the ability of a conventional ASO to reduce expression of

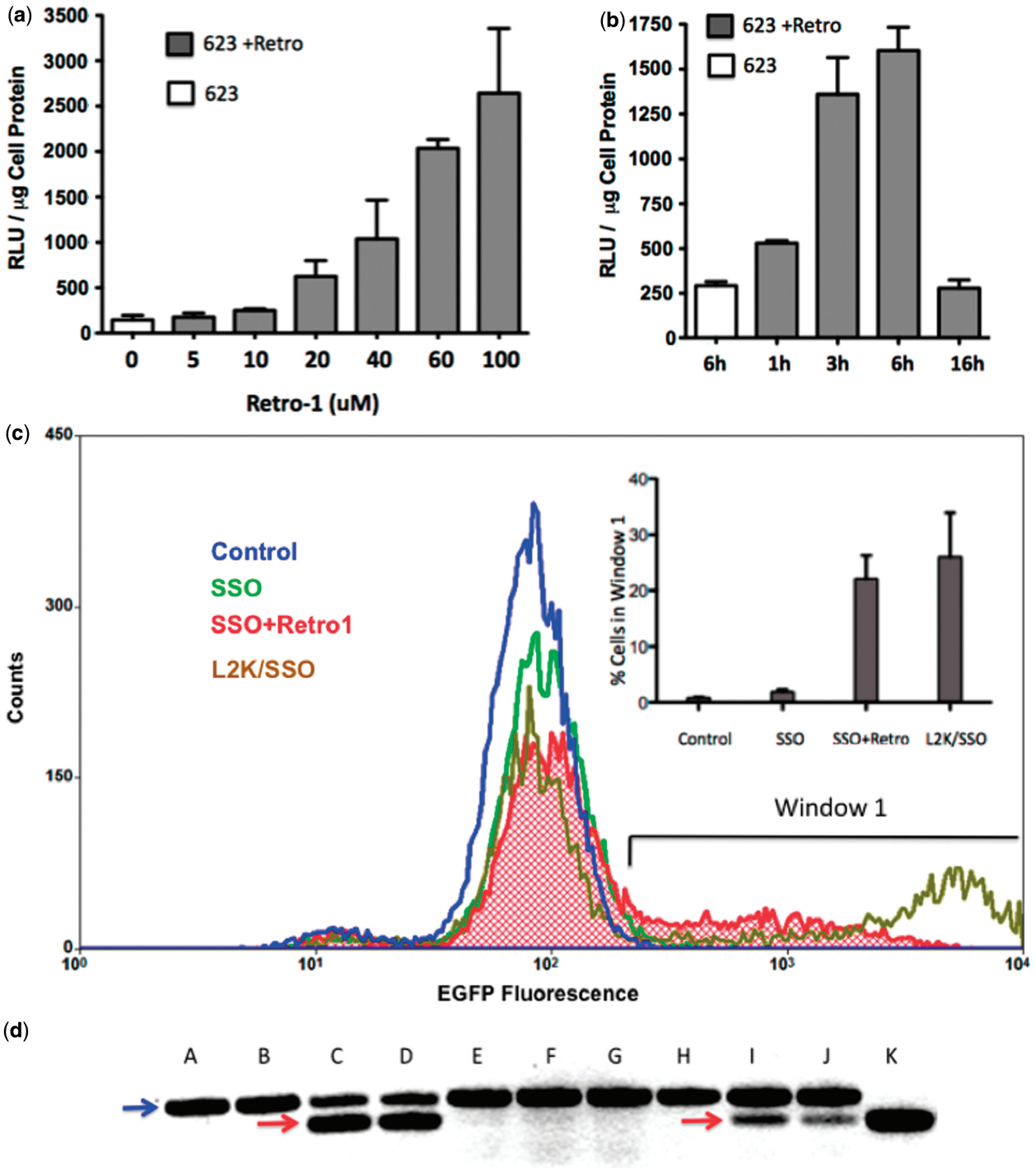

Figure 2. Retro-1 enhances the actions of SSOs. (**a**) Increased luciferase induction with Retro-1 treatment. HeLaLuc705 cells were incubated with 50 nM SSO 623 for 16 h. After removal of the oligonucleotide, the cells were treated (2 h) with various concentrations of Retro-1. After removal of the Retro compound and 6 h further incubation, luciferase activity and cell protein were measured. Grey bars, SSO 623 + Retro-1; open bar, SSO 623 alone. $n = 4$. Means + standard error. (**b**) Time course of luciferase induction. HeLaLuc705 cells were incubated with SSO 623. After removal of the, oligonucleotide the cells were treated (2 h) with 80 µM Retro-1. After removal of the Retro compound, the cells were incubated for various times before harvesting and measurement of luciferase activity and cell protein. Grey bars, SSO 623 + Retro-1 after various times of incubation; open bar, SSO 623 alone after 6 h of incubation. $n = 4$. Means + standard error. (**c**) Increased EGFP induction with Retro-1 treatment. HeLaEGFP654 cells were incubated with SSO 623 with or without subsequent treatment with Retro-1. Additionally, a positive control group received SSO 623 delivered using Lipofectamine 2000 (L2K/SSO). EGFP expression was measured by flow cytometry. Ordinate, cell counts; abcissa, log scale of fluorescence. Blue profile, untreated HelaEGFP654 cells; Green profile, + SSO 623; Red profile, + SSO 623 + 100 µM Retro-1; Brown profile, + SSO 623 + Lipofectamine 2000. The inset shows the percentage of cells in Window 1 (high EGFP expression). $n = 3$. Means + standard error. (**d**) Splice correction at the RNA level. The experiment described in (c) was also analysed by RT-PCR as described in 'Materials and Methods' section. The blue arrow indicates the incorrectly spliced RNA from the EGFP654 reporter, whereas the red arrows indicate the correctly spliced mRNA. A, B = untreated controls; C, D = +SSO 623 + Lipofectamine 2000; E, F = +SSO 623 only; G, H = +Retro-1 only; I, J = +SSO 623 + Retro-1; K = EGFP expressing plasmid.

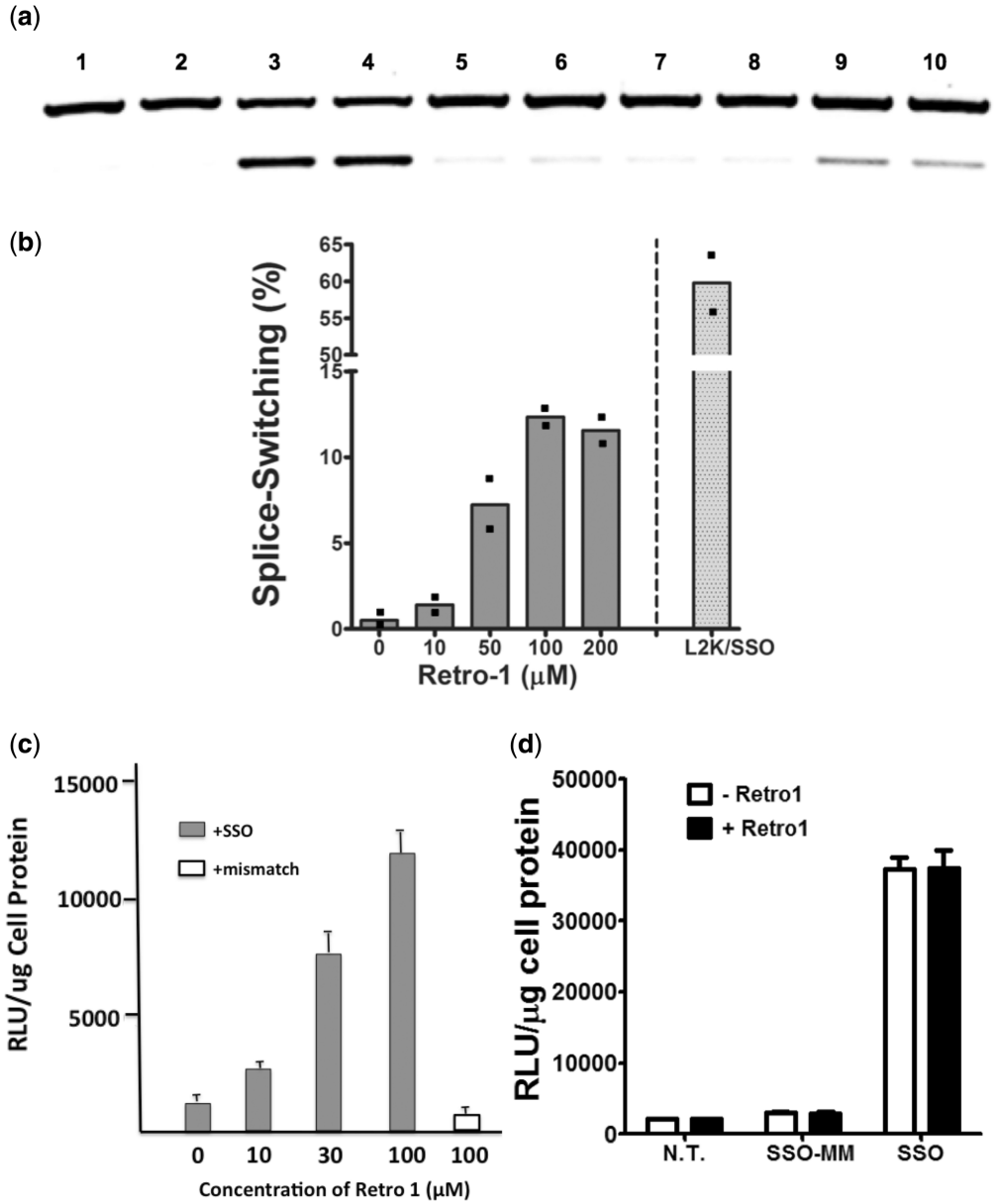

Figure 3. Retro-1 effects on the splicing of an endogenous RNA and exploration of mechanisms. (**a**) Retro-1 enhances SSO effects on an endogenous message. PC3 cells were treated for 16 h with 250 nM of an SSO that shifts the splicing of Bcl-x pre-mRNA to the Bcl-x_S form. Cells were subsequently treated with 100 μM Retro-1 for 2 h or maintained as controls. Cells treated with the SSO complexed with Lipofectamine 2000 provided a positive control. RNA was extracted and analysed by RT-PCR as described in 'Materials and Methods' section. Upper band, Bcl-x_L product; lower band, Bcl-x_S product. Lanes 1,2 untreated control (no SSO); Lanes 3,4 SSO + Lipofectamine 2000; Lanes 5,6 SSO only; Lanes 7,8 Retro-1 only; Lanes 9,10 SSO+ Retro-1. (**b**) Dose-response for Bcl-x splicing modification. In an experiment similar to that of Figure 3a, various concentrations of Retro-1 were tested. Band intensities were quantitated with a gel scanner as described in 'Materials and Methods' section. The ordinate shows the ratio of the Bcl-x_S (lower) band to the total (upper plus lower) band intensity expressed as a percentage. Bars show mean values, individual values shown as black squares. $n = 2$. (**c**) Retro-1 treatment does not cause non-specific increases in splicing activity. A375Luc705 cells were incubated with 50 nM SSO 623 or its mismatch control. After removal of the oligonucleotide, the cells were treated (2 h) with various concentrations of Retro-1. After removal of the Retro compound and further incubation, luciferase activity and cell protein were measured. Grey bars, SSO 623; open bar, mismatch oligonucleotide. $n = 6$. Mean + standard error. (**d**) Retro-1 does not affect the action of oligonucleotides delivered by electroporation. SSO 623 or its mismatch control (SSO-MM) (100 pmoles) were directly delivered to the cytosol of A375Luc705 cells by Amaxa ® electroporation. Thereafter, the cells were treated for 2 h with Retro-1 (100 μM). After removal of the Retro compound, the cells were further incubated and then assayed for luciferase activity and cell protein. Black bar, + Retro-1; white bar, - Retro-1; NT, not treated. $n = 3$. Mean + standard error.

its target. As seen in Figure 4a, treatment of multi-drug-resistant NIH 3T3 cells with 100 nM of a 2′-O-Me phosphorothioate gapmer ASO alone had no effect on expression of Pgp. However, when used in conjunction with 100 μM Retro-1, the antisense oligomer caused a distinct left shift of the flow cytometry profile indicating reduced Pgp expression. As shown in Figure 4b, there was a dose-response relationship, with increasing concentrations of Retro-1 contributing to progressive reductions in Pgp expression. At the highest concentration of Retro-1 tested,

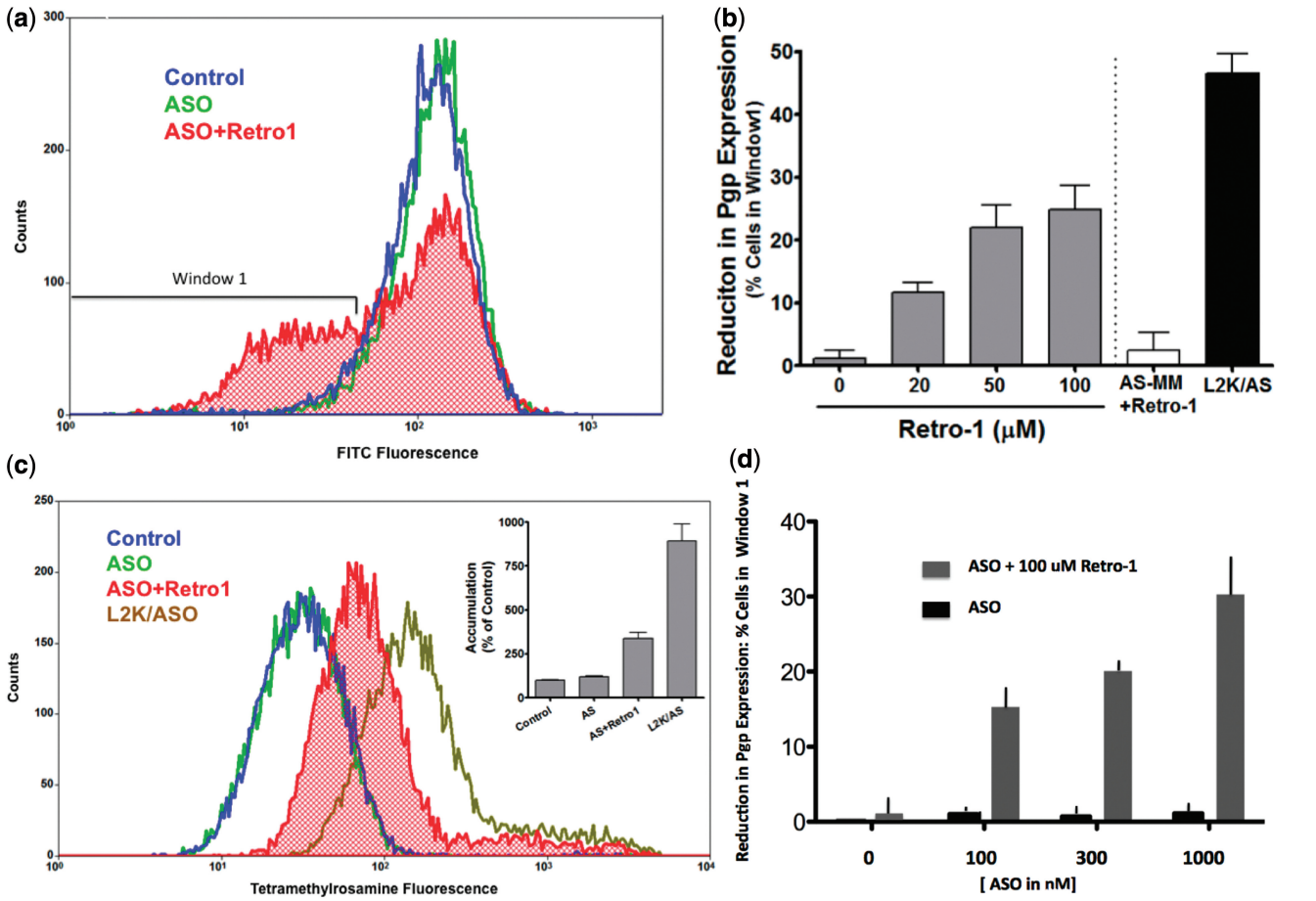

Figure 4. Retro-1 enhances the actions of antisense oligonucleotides. (**a**) Reduction of Pgp expression. NIH-3T3-MDR cells were incubated with 100 nM anti-MDR1 antisense oligonucleotide (ASO). After removal of the ASO, the cells were incubated for 2 h with or without 100 μM Retro-1. After removal of the Retro compound, the cells were further incubated for 48 h and then assayed for cell surface expression of Pgp using a monoclonal antibody and flow cytometry. Reduced Pgp expression is indicated by a left shift of the cytometry profile into window 1. Ordinate, cell counts; abcissa, log scale of fluorescence. Blue profile, untreated MDR cells; Green profile, + ASO; Red profile, + ASO + Retro-1. (**b**) Retro-1 concentration versus response for Pgp reduction. Cells were treated with 100 nM antisense (AS) and with various amounts of Retro-1. Treatment with 100 nM AS and Lipofectamine 2000 (L2K) served as a positive control, whereas treatment with 100 nM mismatched oligonucleotide (AS-MM) and 100 uM Retro-1 served as a negative control. Pgp expression was assayed as in Figure 4a. The ordinate indicates the percentage of the cell population in Window 1. Grey bars, treatment with AS plus Retro-1; White bar, treatment with AS-MM plus 100 μM Retro-1; Black bar, AS plus L2K. $n = 4$. Mean + standard error. (**c**) Increased accumulation of a Pgp substrate. Cells were incubated with 100 nM antisense followed by treatment with 100 μM Retro-1 as in (a), or with 100 nM antisense and Lipofectamine 2000(L2K). After 48 h, cells were exposed to the Pgp substrate tetramethylrosamine for 1 h; dye accumulation was analysed by flow cytometry. Blue profile, control cells; Green profile, + ASO; Red profile, + ASO + Retro-1; Brown profile, + ASO + Lipofectamine 2000. Inset: Mean value of tetramethylrosamine fluorescence as percentage of untreated control. $n = 4$. Mean + standard error. (**d**) Antisense Concentration-Response for Pgp reduction. NIH-3T3-MDR cells were incubated with various concentrations of anti-MDR1 oligonucleotide. After removal of the ASO, some of the samples were incubated with 100 μM Retro-1 for 2 h followed by removal of the Retro compound and further incubation. Pgp expression was measured by immunostaining and flow cytometry. Ordinate, percentage of total cells in the low Pgp window; abcissa, concentration of antisense oligonucleotide. $n = 3$. Mean + standard error.

the reduction in Pgp expression was about one half of that obtained using an optimal amount of cationic lipid (~25% versus 45% reduction); thus, the Retro-1 effect is reasonably robust. The combination of antisense and Retro-1 also caused functional changes in terms of decreased ability of the drug-resistant cells to export a fluorescent Pgp substrate (Figure 4c). We also used the Pgp assay to evaluate the relationship between antisense concentration and Retro compound effects. As seen in Figure 4d, increasing concentrations of the ASO alone had little effect on Pgp, but the presence of the Retro compound allowed a progressive ASO concentration-dependent reduction of Pgp expression.

Using the same model, we evaluated the ability of Retro-1 to influence the pharmacological action of a siRNA (Supplementary Figure S3 and Supplementary Table S1). Thus, multi-drug resistant NIH 3T3 cells were treated with MDR1 siRNA or ASO with or without subsequent treatment with Retro-1. Additionally, complexes of ASO or siRNA with cationic lipids were tested. As seen in the supplementary data, there was a major reduction of Pgp expression when 100 nM of either ASO or siRNA were delivered using cationic lipid. There was also a distinct reduction in Pgp expression when a combination of 100 nM ASO and Retro-1 was used. However, treatment with 1000 nM siRNA plus Retro-1 failed to reduce Pgp

expression. Thus, Retro-1 failed to enhance siRNA effects when the siRNA was used at pharmacologically meaningful (sub-micromolar) concentrations. One possible explanation of these results is that that siRNAs may traffic differently than ASOs, using pathways not affected by Retro-1. An alternative explanation of this negative result is that the initial cellular uptake of conventional siRNA is much lower than that of phosphorothioate-modified ASO and SSO oligonucleotides. For example, in comparing uptake of an siRNA and an SSO, both labelled with the same fluorophore, we found that uptake of the siRNA was <5% that of the SSO (data not shown). Additionally, conventional siRNAs are less stable to cellular nucleases than are phosphorothioate SSOs and ASOs, and this may contribute to the lack of effect.

To make sure that the effects of Retro-1 on antisense actions are not confined to a single sequence, we examined a second target, namely the apototic regulator Bcl-X_L. These experiments made use of a published anti Bcl-X_L sequence and control mismatch sequence (44). As seen in Supplementary Figure S4, the use of Retro-1 augmented the antisense-mediated reduction of message. In this case, Retro plus antisense treatment resulted in ~40% reduction in message levels, whereas use of a cationic lipid resulted in ~90% reduction, both as compared with antisense alone. The control mismatch sequence was inactive even when delivered using cationic lipid transfection.

The concentrations of Retro-1 used in the experiments described in Figures 2–4 had little effect on viability of HeLa or A375 cells. Nor did they affect the integrity of the plasma membrane as determined using a lactate dehydrogenase release assay (54) (see Supplementary Figure S5a and b). Thus, the observed effects on splice correction and antisense activity cannot be ascribed to toxicity or overall loss of membrane integrity.

Retro-1 selectively alters the intracellular distribution of oligonucleotides

The pharmacological actions of antisense and SSOs are usually correlated with delivery to the nucleus (26,55). Thus, we examined the effect of Retro-1 on nuclear localization of a fluorophore-labelled SSO. As seen in Figure 5a, in the control situation, oligonucleotide fluorescence was confined to cytoplasmic vesicles with no evidence of nuclear accumulation. However, in the cells treated with Retro-1, in addition to the vesicular fluorescence, there was clearly evident nuclear fluorescence. As single-stranded oligonucleotides can readily move from the cytosol to the nucleus (56), the increased nuclear fluorescence observed in the presence of the Retro agent is likely due to partial release of the oligonucleotide from vesicular compartments to the cytosol.

To further pursue this issue, we have used chimeras of GFP with marker proteins for specific endomembrane compartments to visualize the subcellular distribution of oligonucleotides in live cells and to quantify changes caused by Retro-1. For example, as seen in Figure 5b, just before the addition of Retro-1, there was considerable co-localization of fluorescent oligonucleotide with Rab 9, a late endosome marker protein that is thought to be involved in endosome to TGN trafficking (40). In contrast, at this point in the oligonucleotide uptake process, there was little co-localization of fluorescent oligonucleotide with Rab 5 or Rab 11, markers for early and recycling endosomes, respectively (57), nor with *N*-acetylgalactosaminyltransferase 2, a marker for the Golgi (58) (Figure 5c).

We then examined the kinetics of changes in the co-localization of a fluor-labelled oligonucleotide with protein markers of key endomembrane compartments upon exposure to Retro-1. As seen in Figure 6, the addition of Retro-1 resulted in a rapid decrease in co-localization of the fluorescent oligonucleotide with the late endosomal markers Rab 7 and Rab 9. This was accompanied by a rapid increase in the accumulation of oligonucleotide in the nucleus. In contrast, although there was considerable initial co-localization of oligonucleotide with the lysosomal marker LAMP-1 (59), little change in co-localization was observed on addition of Retro-1. We interpret these observations as indicating release of oligonucleotide from Rab 7/9 positive compartments, but not from LAMP-1 positive lysosomes. The observation that Retro-1 caused a rapid redistribition of oligonucleotide from endomembrane compartments to the nucleus prompted us to more closely examine the kinetics of Retro effects on splice modification. Thus, as seen in Supplementary Figure S6, even a very brief (5 min) treatment with Retro-1 caused a substantial increase in splicing modification as detected by luciferase induction, whereas the effect increased progressively up to 90-min exposure. This is very consistent with the kinetics of oligonucleotide relocalization seen in Figure 6. These observations suggest that exposure of cells to Retro-1 results in a rapid partial destabilization of a subset of endomembrane compartments, particularly late endosomes, with consequent release of entrapped oligonucleotide to the cytosol and nucleus.

To confirm that there were negligible effects of Retro-1 on lysosomes, we examined the cellular accumulation of the lysosomotropic dye LysoTracker Green® in cells treated with Retro-1, or with chloroquine, a drug that increases the pH of lysosomes and causes release of lysosomal contents to the cytosol (30,60). As seen in Figure 7a, chloroquine treatment markedly reduced cellular accumulation of LysoTracker Green®, whereas a pharmacologically effective concentration of Retro-1 had little effect, indicating a lack of lysosomotropic action. We further pursued this issue by examining changes in co-localization of a fluorescent oligonucleotide with the lysosomal marker protein LAMP-1 subsequent to treatment with Retro-1 or chloroquine. As seen in Figure 7b, chloroquine, but not Retro-1, resulted in reduced colocalization of the oligonucleotide and the lysosomal marker. In Figure 7c, individual images are presented further illustrating that Retro-1 affects colocalization of fluorescent oligonucleotide with the late endosomal marker Rab 7, but not the lysosomal marker LAMP-1.

Thus, as indicated by the original observations on toxin trafficking (41), Retro-1 is selective and affects only a restricted subset of endomembrane compartments. Our observations suggest that Retro-1 causes partial

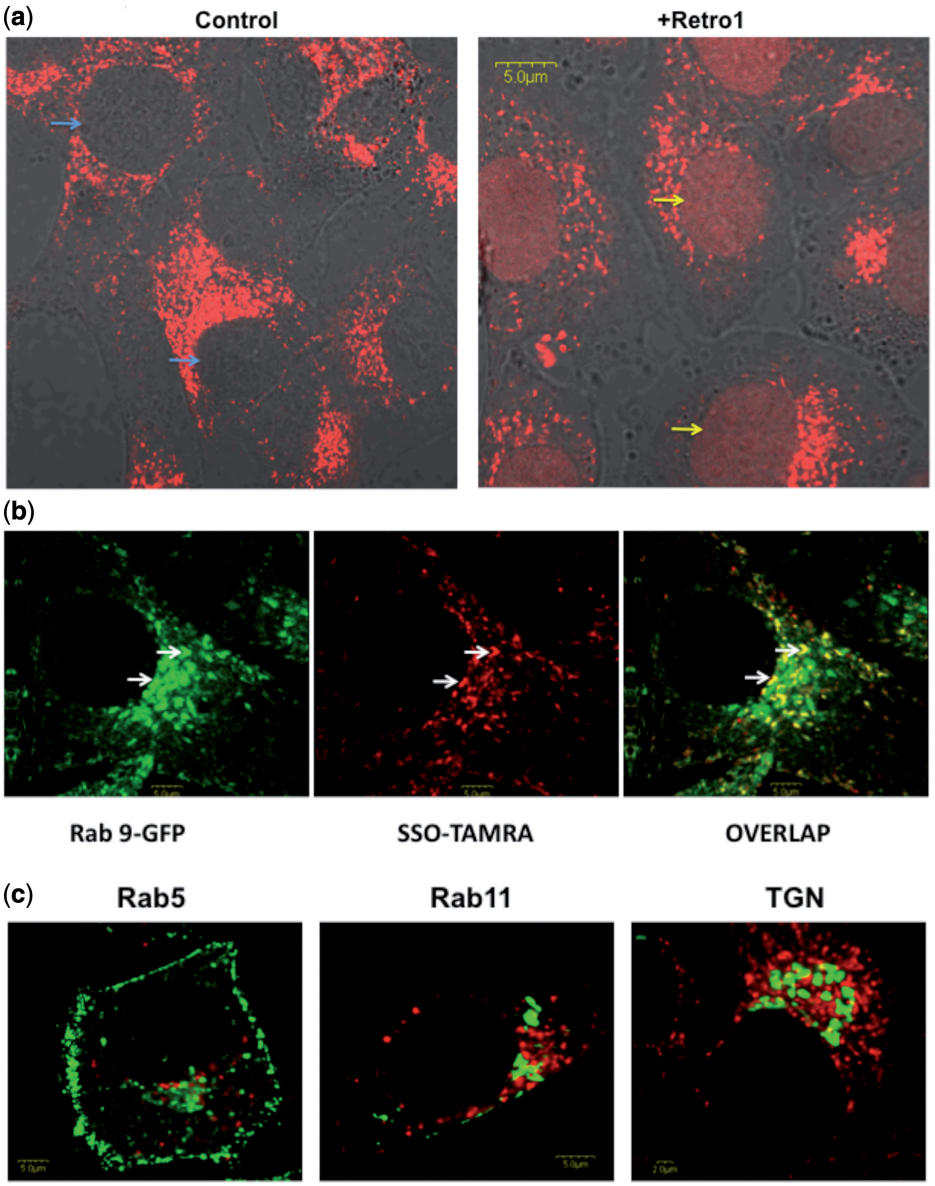

Figure 5. Retro-1 causes subcellular redistribution of oligonucleotides. (**a**) Increased nuclear accumulation of oligonucleotide. HeLa cells on cover glasses were incubated with 200 nM 3′-TAMRA conjugated SSO 623 for 24 h with or without subsequent treatment with 100 µM Retro-1 for 2 h. Live cells were observed by confocal microscopy. Blue arrows indicate typical 'empty' nuclei. Yellow arrows indicate typical nuclei containing oligonucleotide. (**b**) Co-localization of oligonucleotide with Rab 9. HeLa cells were transfected with a plasmid encoding a GFP chimera of Rab 9. The transfection agent was removed by rinsing with serum, and the cells maintained in growth medium for 24 h. Thereafter, cells were incubated with 200 nM 3′-TAMRA conjugated SSO 623 for 24 h. Live cells were observed by confocal microscopy. Green image, GFP fluorescence. Red image, TAMRA fluorescence. White arrows indicate typical distinct subcellular structures that show co-localization of Rab 9 and oligonucleotide. (**c**) Lack of co-localization with early endosome or Golgi markers. HeLa cells were transfected with GFP chimeras that serve as markers for several endomembrane compartments (Rab 5, early endosomes; Rab 11, recycling endosomes; *N*-acetylgalactosaminyltransferase 2, TGN). Thereafter, cells were incubated with 200 nM 3′-TAMRA conjugated SSO 623 for 24 h. Live cells were observed by confocal microscopy. Green image, GFP fluorescence. Red image, TAMRA fluorescence.

destabilization of Rab 7/9 positive compartments, thus allowing release of entrapped oligonucleotide to the cytosol and thence the nucleus. However, unlike lysosomotropic agents, Retro-1 does not cause destabilization of lysosomes.

Retro-1 enhances the actions of SSOs *in vivo*

We have performed an initial evaluation of the *in vivo* effects of Retro-1 on the pharmacological actions of SSOs. We used xenografts of the A375Luc705 human melanoma cells aforementioned. These cells were implanted into NOD *scid* mice and allowed to form tumours. The tumour-bearing mice were treated by intraperitoneal injection with SSO 623 or with phosphate buffered saline (PBS), and a cohort was subsequently treated intravenously with Retro-1. The mice were imaged for luciferase induction at several points in this process. As seen in Figure 8a, unlike the situation in cell culture, there was a high

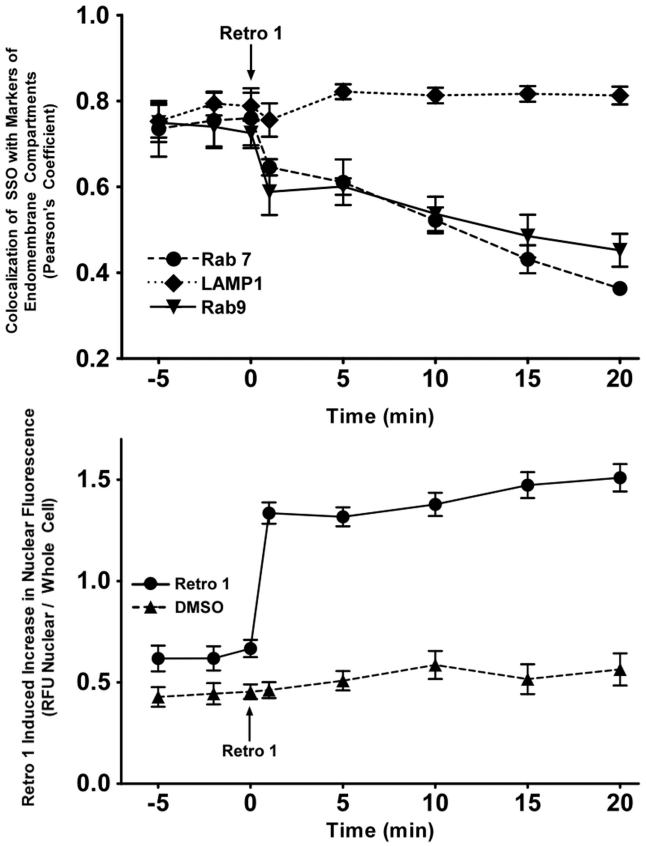

Figure 6. Retro-1 selectively affects distinct endomembrane compartments. Kinetics of Retro-1 effects on the subcellular localization of oligonucleotide. HeLa cells were transfected with plasmid or baculovirus expression vectors for GFP chimeras of the late endosomal markers Rab 9, Rab 7 or the lysosomal marker LAMP-1. After removal of the vectors and 24 h additional culture, cells were exposed to 200 nM 3′-TAMRA conjugated SSO 623 for 6 h and then rinsed to remove excess oligonucleotide. Live cells were observed and analysed using confocal fluorescence microscopy as described in 'Materials and Methods' section. Upper panel: Colocalization of GFP and TAMRA-SSO over timed intervals before and after the addition of Retro-1, quantitated as described in 'Materials and Methods' section. Lower panel: the ratio of nuclear to cytosolic TAMRA-SSO quantitated over timed intervals before and after the addition of Retro-1. Results shown: means ± standard errors. N ranges from 7 to 31 individual observations.

background level of spontaneous splice correction and luciferase induction in the tumours. Before Retro-1 administration, the animals receiving the SSO 623 displayed luciferase levels no different from the PBS controls. However, subsequent to Retro-1 administration, the SSO 623+ Retro-1 cohort displayed an increase in luminescence as compared with PBS controls or the cohort treated with SSO623 alone. Analysis of splice correction in the tumours by reverse transcriptase-polymerase chain reaction (RT-PCR) is shown in Figure 8b and c and confirms the results obtained by imaging, namely that there is a small, but distinct, splice correction seen in the SSO+Retro-1 treated samples. Biochemical measurement of luciferase activity in tumour samples also gave similar results (Figure 8d). Thus, three different assays indicated a modest (~2-fold), but distinct, *in vivo* effect of Retro-1 treatment.

As part of these studies, we used blood samples to examine clinical chemistry parameters that might reflect possible toxicities. As seen in Supplementary Figure S7, the toxicities displayed by SSO 623 and Retro-1 were limited. Thus, the only significant difference was a moderate elevation in plasma alanine aminotransferase levels in the SSO 623 treated mice possibly reflecting some liver toxicity. These results agree well with previous observations indicating the Retro-1 has little *in vivo* toxicity (41).

An issue with these *in vivo* studies is that, at present, we have no information about the pharmacokinetics and biodistribution of Retro-1. Thus, it is difficult to match the well-known pharmacokinetic and biodistribution behaviour of the oligonucleotides with that of Retro-1 so as to optimize effectiveness of the combination. Retro-1 is very poorly water soluble; thus, for *in vivo* studies, we administered it in a mixture of DMSO/PEG400. In view of its poor solubility, it is possible some of the drug became insoluble after injection, and that only very low concentrations were attained in the tumours, and thus luciferase induction was correspondingly poor. However, although the magnitude of the effects observed thus far are modest, it is clear that Retro-1 can enhance *in vivo* actions of SSOs to some extent.

DISCUSSION

The development of non-toxic small molecules with the ability to significantly enhance the pharmacological actions of oligonucleotides would clearly have important therapeutic ramifications. The studies presented here are essentially a proof of principle for that possibility. Thus, we have shown that the novel compound Retro-1 can increase the effects of SSOs and ASOs in the cell culture context. We have also demonstrated that Retro-1 can modestly improve the actions of a SSO *in vivo*. The magnitude of the enhancement attained in cell culture with Retro-1 is less than that which can be attained by delivery of oligonucleotides using cationic lipid complexes, but nonetheless is substantial. Although neither the oligonucleotides used in this study nor Retro-1 are entirely free of toxic effects, the observed toxicities seem relatively mild at both the cellular and whole animal levels. As Retro-1 is effective in enhancing oligonucleotide actions only at micromolar concentrations and is also poorly water soluble, it may not be useful in the therapeutic context itself. However, our experience with this compound, whose effects on oligonucleotides were discovered in a serendipitous manner, strongly suggests that it should be possible to systematically develop more potent non-lysosomotropic, non-toxic small molecules capable of enhancing oligonucleotide actions by affecting their intracellular processing.

Retro-1 was first identified as an agent that interferes with the intracellular trafficking of toxins (41). We became interested in this molecule because studies from our laboratory and others have shown that the pathway

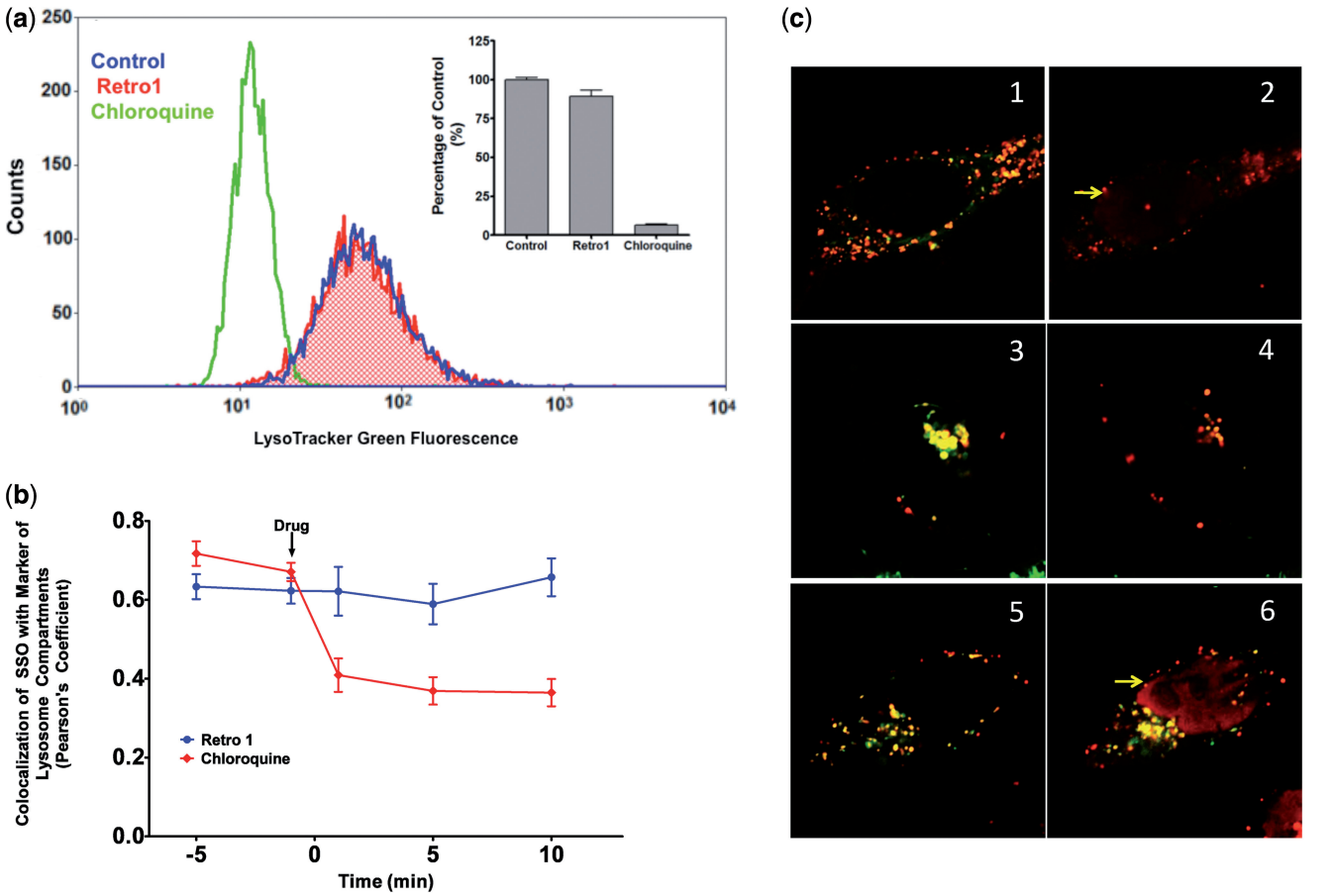

Figure 7. Retro-1 does not affect lysosomes. (**a**). Retro-1 does not affect accumulation of a lysosomotropic dye. A375 cells were treated with 100 μM Retro-1 or 100 μM chloroquine for 2 h. Thereafter, 100 nM LysoTracker Green was added. After 30 m, uptake of the dye was monitored by flow cytometry with a 488-nm laser coupled with a 525/50 filter. The ordinate is cell counts; the abcissa is Lysotracker fluorescence. Blue profile, control cells; Green profile, chloroquine-treated cells; Red profile, Retro-1-treated cells. Inset: mean fluorescence as percentage of untreated control. $n = 3$. Means + standard error. (**b**) Chloroquine, but not Retro-1, affects co-localization of oligonucleotide with a lysosomal marker protein. HeLa cells were transfected with a baculovirus expression vector for a GFP chimera of LAMP-1 a lysosomal marker protein. After 24 h culture, cells were exposed to 200 nM 3′-TAMRA conjugated SSO 623 for 6 h and then rinsed to remove excess oligonucleotide. Cells were then treated with 100 μM Retro-1 or 300 uM chloroquine. Live cells were observed using confocal fluorescence microscopy. The panel shows colocalization of GFP-Lamp-1 and TAMRA-SSO over timed intervals before and after the addition of drug, quantitated as described in 'Materials and Methods' section. Means and standard errors shown. $n = 7$. (**c**) Images of cell treated with Retro-1 or chloroquine. Co-localization of TAMRA-SSO and GFP chimeras is indicated by the yellow/orange signal. Cells expressing GFP-Rab7 before [1] or after [2] Retro-1 treatment, showing reduced co-localization. Cells expressing GFP-LAMP1 before [3] or after [4] chloroquine treatment, showing reduced co-localization. Cells expressing GFP-LAMP1 before [5] or after [6] Retro-1 treatment, showing persistence of co-localization. Nuclei showing increased accumulation of the SSO owing to Retro-1 treatment are marked by yellow arrows.

of uptake and trafficking of oligonucleotides can influence their pharmacological effectiveness (26,36,37). However, unlike lysosomotropic agents, or cationic lipids or polymers, the effects of Retro-1 on sub-cellular organization and intracellular trafficking are subtle (41). Treatment with Retro-1 does not disrupt the overall organization of the endosome-lysosome system, nor the endoplasmic reticulum or the Golgi apparatus. Moreover, although toxin trafficking is blocked, other intracellular trafficking processes remain intact. The exact molecular targets of Retro-1 are not yet known, but in terms of toxin trafficking, it seems to act at the functional interface between endosomes and the TGN, most probably at the retromer level. At this point, it is not clear whether the effects of Retro-1 on toxin trafficking and on oligonucleotide redistribution share the same fundamental mechanism or whether the oligonucleotide effects involve a distinct molecular target.

Our studies add a new aspect to the functions of Retro-1. This molecule clearly causes a rapid partial release of oligonucleotides from a subset of endomembrane compartments where they have accumulated but are pharmacologically inert, and allows oligonucleotides to gain entry into the cytosol and then the nucleus. As it requires some time for oligonucleotides to reach the cellular site where they are influenced by Retro-1, this suggests that a 'deep' endosomal compartment is involved. The effects of Retro compounds on the morphology of subcellular organelles are subtle; thus, it has been challenging to definitively identify the endomembrane compartment(s) from which the oligonucleotides are released. However, our results strongly suggest that Rab 7 - and Rab 9-positive endosomes are an

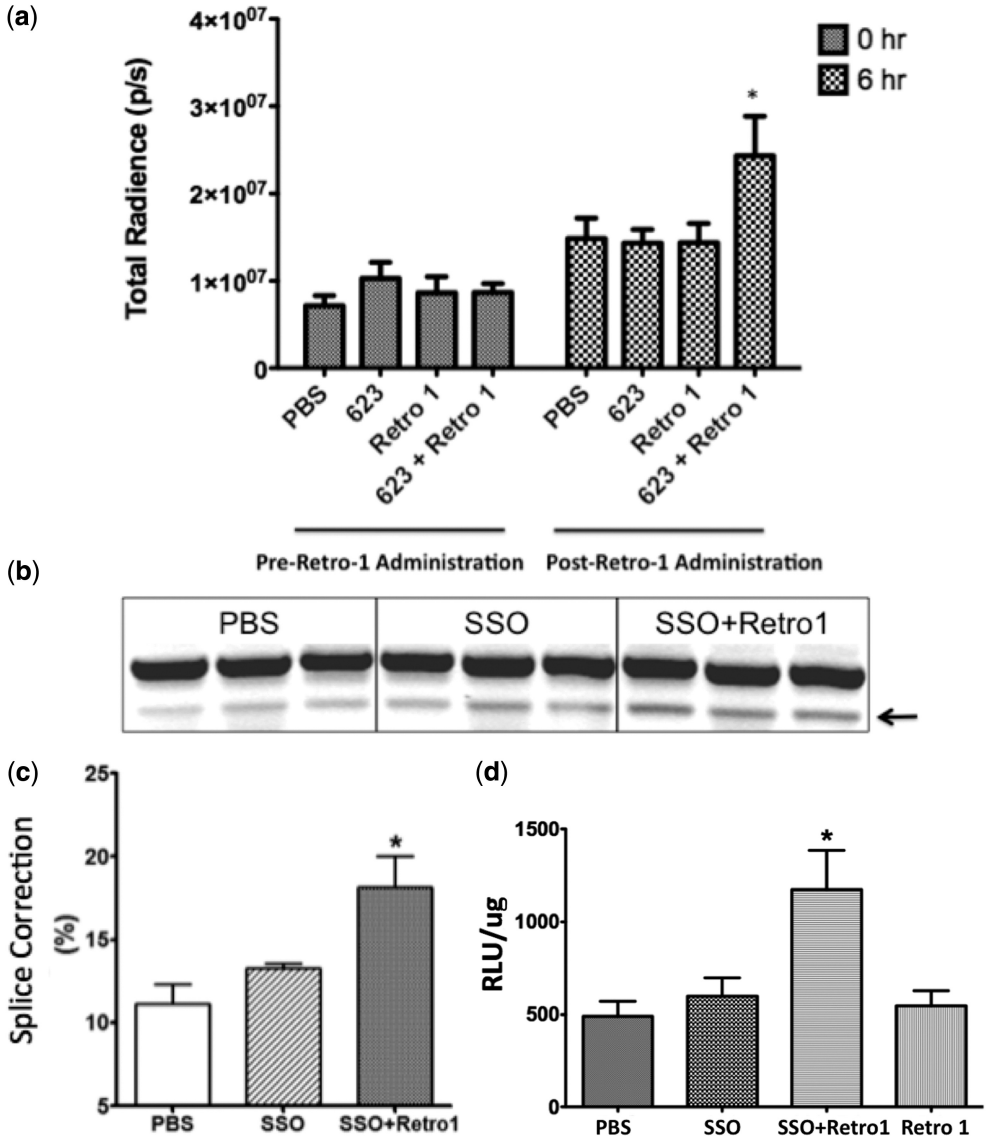

Figure 8. Retro-1 effects *in vivo*: xenograft experiments. NOD *scid* mice received bilateral sub-cutaneous xenografts of 2×10^6 A375Luc705 human melanoma cells. After tumour growth, mice received intra-peritoneal injections of PBS or of SSO623 in PBS. At 18 h after the last intraperitoneal injection, the mice were imaged for luciferase activity. Immediately, thereafter a cohort of the PBS control mice and a cohort of the SSO623 mice received a single 40 µl intra-venous injection of 2 mg of Retro-1. The mice were re-imaged 6 h after that injection. (**a**) Quantitation of luminescence. This displays the luminescence (total radiance) before and 6 h after the injection of Retro-1. The groups were as follows: PBS only; SSO623 only; PBS followed by Retro-1; SSO623 followed by Retro-1. Means and standard deviations are shown. $n = 10$. The 623 plus Retro group was the only one where luminescence was significantly elevated from the PBS control group ($P < 0.05$). The slight increase in luminescence seen in all groups between t = 0 and t = 6 h is likely due to the persistence of small amounts of luciferin in the tissues from the $t = 0$ imaging session (http://invivoimaging-community.com/luciferin_protocol). (**b**) Analysis of splice correction. RT-PCR and gel analysis was performed to monitor the levels of correctly and incorrectly spliced RNA produced by the Luc705 reporter. Correctly spliced Luc mRNA is marked by an arrow. (**c**) Quantitation of splice correction. This shows the percentage of splice correction determined by measuring band intensities. $n = 3$. Means + standard error. The SSO623 + Retro-1 samples were significantly different from the PBS controls ($P < 0.05$). (**d**) Luciferase activity in xenografts. Tumour samples from the xenograft experiment were homogenized and then analysed for luciferase activity and total protein as described in 'Materials and Methods' section. The SSO623 + Retro-1 samples were significantly different from the PBS controls ($P < 0.05$). $n = 4$–7. Means + standard errors.

important source of pharmacologically active oligonucleotide in Retro-1-treated cells. In contrast, Retro-1 does not release oligonucleotides from lysosomes, thus differentiating it from the class of small molecule lysosomotropic agents such as chloroquine, and from polymeric nanocarriers that act by the 'proton sponge' effect (61). One might hypothesize that there would be advantages to using compounds that can release oligonucleotides from endomembrane compartments but that do not cause release of lysosomal hydrolases to the cytosol, and the toxicities of Retro-1 seem rather mild. However, the relative toxicities of manipulating endosomal verus lysosomal compartments remain unknown at this point.

As the actions of ASOs and SSOs are both influenced by Retro-1, it seems likely that a portion of both types of oligomers are accumulating in the key compartment(s) that is affected by the drug. However, the intracellular trafficking of oligonucleotides is likely to be complex and influenced by characteristics such as oligomer size and charge. For example, we do not know whether our current findings would also extend to oligomers that have uncharged backbones such as morpholino oligonucleotides or peptide nucleic acids (6,62–64). Similarly, our observation that Retro-1 failed to enhance the action of a siRNA may be due to the use of alternative trafficking pathways by single- and double-stranded oligonucleotides, or may more simply be explained by the very low cellular uptake of conventional siRNAs and their relative instability in the cellular milieu. Thus, it would be interesting to determine whether the newly described phosphorothioate modified single-stranded siRNAs that chemically resemble ASOs are affected by Retro-1 (65).

An important issue yet to be explored is whether Retro-1 affects ligand-conjugated oligonucleotides that can target specific cell surface receptors (66). There has been great progress recently in using peptides, aptamers and small molecule conjugates to enhance both the specificity and the magnitude of oligonucleotide delivery (21,24,39,66,67). Our previous work has suggested that ligand conjugated SSOs and unconjugated SSOs follow different uptake pathways (36). Thus, it is unclear whether various types of oligonucleotide conjugates will traffic through the subcellular compartments affected by Retro-1. If that were the case, however, it would set up a potentially powerful synergy, with ligand conjugation providing specificity and enhanced cellular uptake, and Retro-1 or similar small molecule adjuncts providing improved release from non-productive endomembrane compartments to the cytosol.

Our *in vivo* studies indicate that Retro-1 can modulate oligonucleotide effects in tumours. The increased luciferase induction in xenografts manifested by treatment with Retro-1 plus the SSO was modest. There was a high background luminescence in this situation, and the enhancement observed was about twice the level of the buffer-treated controls. However, previous studies were unable to attain any response whatsoever to SSOs in xenografts unless strong cationic transfection agents were used (46,68). Thus, the ability of Retro-1 to evoke a response in this challenging context is interesting. Our *in vivo* studies also indicated that the toxicity of administering Retro-1 plus oligonucleotide was minimal with a moderate elevation of a liver enzyme being the only significant difference from the controls. The effects of Retro-1 *in vivo* observed thus far are probably too limited to be of therapeutic significance. However, they suggest the merit of seeking novel compounds with greater potency and efficacy.

Other studies have identified small molecules that influence the action of oligonucleotides. For example, recent reports describe compounds that specifically affect liver miR-122 (69) or that inhibit siRNA loading on to the RISC complex (70). Another approach that is being pursued is the design of non-coding RNAs that can be regulated by small molecules (71). A recent study in muscle cells and tissues showed that Dantrolene, an antagonist of the sarcoplasmic reticulum calcium channel, could directly enhance SSO-mediated splicing, presumably by affecting nuclear calcium levels (72). However, to our knowledge, the current report is the first to describe the enhancement of oligonucleotide action through modulation of intracellular trafficking or processing by a non-lysosomotropic effect.

In summary, Retro-1 substantially enhanced the pharmacologic actions of certain types of commonly used oligonucleotides via a novel mechanism involving release from selected endomembrane stores and redistribution to sites of action in the nucleus. Our observations provide an important proof of principle that non-toxic small molecules can be used to enhance oligonucleotide actions through highly selective modulation of intracellular processing. Because of its relatively low potency and poor water solubility, Retro-1 itself may not be suitable for use as a drug. However, it seems likely that new compounds of greater potency could emerge either via high throughput screening or by chemical optimization and rational design. The development of such compounds could have a transformative effect on the use of oligonucleotides as therapeutic agents.

SUPPLEMENTARY DATA

Supplementary Data are available at NAR Online: Supplementary Table 1 and Supplementary Figures 1–7.

ACKNOWLEDGEMENTS

The authors thank Charlene Ross-Santos and her staff for expert assistance with animal experiments and Md. Rowshon Alam for large-scale oligonucleotide synthesis.

FUNDING

Funding for open access charge: National Institutes of Health grant [R01 CA151964 to R.L.J.]; Commissariat à l'énergie atomique et aux énergies alternatives (to D.G., J.B., J.C.C. and R.N.).

Conflict of interest statement. None declared.

REFERENCES

1. Moazed,D. (2009) Small RNAs in transcriptional gene silencing and genome defence. *Nature*, **457**, 413–420.
2. Ketting,R.F. (2011) The many faces of RNAi. *Dev. Cell*, **20**, 148–161.
3. Bennett,C.F. and Swayze,E.E. RNA targeting therapeutics: molecular mechanisms of antisense oligonucleotides as a therapeutic platform. *Annu. Rev. Pharmacol. Toxicol.*, **50**, 259–293.
4. Sazani,P. and Kole,R. (2003) Therapeutic potential of antisense oligonucleotides as modulators of alternative splicing. *J. Clin. Invest.*, **112**, 481–486.
5. Burnett,J.C., Rossi,J.J. and Tiemann,K. (2011) Current progress of siRNA/shRNA therapeutics in clinical trials. *Biotechnol. J.*, **6**, 1130–1146.
6. Kole,R., Krainer,A.R. and Altman,S. (2012) RNA therapeutics: beyond RNA interference and antisense oligonucleotides. *Nat. Rev. Drug Discov.*, **11**, 125–140.

7. Vaishnaw,A.K., Gollob,J., Gamba-Vitalo,C., Hutabarat,R., Sah,D., Meyers,R., de Fougerolles,T. and Maraganore,J. (2010) A status report on RNAi therapeutics. *Silence*, **1**, 14.
8. Watts,J.K. and Corey,D.R. (2012) Silencing disease genes in the laboratory and the clinic. *J. Pathol.*, **226**, 365–379.
9. Whitehead,K.A., Langer,R. and Anderson,D.G. (2009) Knocking down barriers: advances in siRNA delivery. *Nat. Rev. Drug Discov.*, **8**, 129–138.
10. Juliano,R., Bauman,J., Kang,H. and Ming,X. (2009) Biological barriers to therapy with antisense and siRNA oligonucleotides. *Mol. Pharm.*, **6**, 686–695.
11. Caruthers,M.H. (2011) A brief review of DNA and RNA chemical synthesis. *Biochem. Soc. Trans.*, **39**, 575–580.
12. Davis,M.E., Zuckerman,J.E., Choi,C.H., Seligson,D., Tolcher,A., Alabi,C.A., Yen,Y., Heidel,J.D. and Ribas,A. (2010) Evidence of RNAi in humans from systemically administered siRNA via targeted nanoparticles. *Nature*, **464**, 1067–1070.
13. Love,K.T., Mahon,K.P., Levins,C.G., Whitehead,K.A., Querbes,W., Dorkin,J.R., Qin,J., Cantley,W., Qin,L.L., Racie,T. *et al.* Lipid-like materials for low-dose, in vivo gene silencing. *Proc. Natl Acad. Sci. USA*, **107**, 1864–1869.
14. Schroeder,A., Levins,C.G., Cortez,C., Langer,R. and Anderson,D.G. (2010) Lipid-based nanotherapeutics for siRNA delivery. *J. Intern. Med.*, **267**, 9–21.
15. Tseng,Y.C., Mozumdar,S. and Huang,L. (2009) Lipid-based systemic delivery of siRNA. *Adv. Drug Deliv. Rev.*, **61**, 721–731.
16. Szoka,F. (2008) Molecular biology. The art of assembly. *Science*, **319**, 578–579.
17. Nguyen,J. and Szoka,F.C. (2012) Nucleic acid delivery: the missing pieces of the puzzle? *Acc. Chem. Res.*, **45**, 1153–1162.
18. Coursindel,T., Jarver,P. and Gait,M.J. (2012) Peptide-based in vivo delivery agents for oligonucleotides and siRNA. *Nucleic Acid Ther.*, **22**, 71–76.
19. van den Berg,A. and Dowdy,S.F. (2011) Protein transduction domain delivery of therapeutic macromolecules. *Curr. Opin. Biotechnol.*, **22**, 888–893.
20. Ezzat,K., Andaloussi,S.E., Zaghloul,E.M., Lehto,T., Lindberg,S., Moreno,P.M., Viola,J.R., Magdy,T., Abdo,R., Guterstam,P. *et al.* (2011) PepFect 14, a novel cell-penetrating peptide for oligonucleotide delivery in solution and as solid formulation. *Nucleic Acids Res.*, **39**, 5284–5298.
21. Dassie,J.P., Liu,X.Y., Thomas,G.S., Whitaker,R.M., Thiel,K.W., Stockdale,K.R., Meyerholz,D.K., McCaffrey,A.P., McNamara,J.O. 2nd and Giangrande,P.H. (2009) Systemic administration of optimized aptamer-siRNA chimeras promotes regression of PSMA-expressing tumors. *Nat. Biotechnol.*, **27**, 839–849.
22. Alam,M.R., Ming,X., Fisher,M., Lackey,J.G., Rajeev,K.G., Manoharan,M. and Juliano,R.L. (2011) Multivalent cyclic RGD conjugates for targeted delivery of small interfering RNA. *Bioconjug. Chem.*, **22**, 1673–1681.
23. Yamada,T., Peng,C.G., Matsuda,S., Addepalli,H., Jayaprakash,K.N., Alam,M.R., Mills,K., Maier,M.A., Charisse,K., Sekine,M. *et al.* (2011) Versatile site-specific conjugation of small molecules to siRNA using click chemistry. *J. Org. Chem.*, **76**, 1198–1211.
24. Sethi,D., Chen,C.P., Jing,R.Y., Thakur,M.L. and Wickstrom,E. (2012) Fluorescent peptide-PNA chimeras for imaging monoamine oxidase A mRNA in neuronal cells. *Bioconjug. Chem.*, **23**, 158–163.
25. Akhtar,S. (2010) Cationic nanosystems for the delivery of small interfering ribonucleic acid therapeutics: a focus on toxicogenomics. *Expert Opin. Drug Metab. Toxicol.*, **6**, 1347–1362.
26. Juliano,R.L., Ming,X. and Nakagawa,O. (2011) Cellular uptake and intracellular trafficking of antisense and siRNA oligonucleotides. *Bioconjug. Chem.*, **23**, 147–157.
27. Varkouhi,A.K., Scholte,M., Storm,G. and Haisma,H.J. (2011) Endosomal escape pathways for delivery of biologicals. *J. Control Release*, **151**, 220–228.
28. Doherty,G.J. and McMahon,H.T. (2009) Mechanisms of endocytosis. *Annu. Rev. Biochem.*, **78**, 857–902.
29. Howes,M.T., Mayor,S. and Parton,R.G. (2010) Molecules, mechanisms, and cellular roles of clathrin-independent endocytosis. *Curr. Opin. Cell Biol.*, **22**, 519–527.
30. Khalil,I.A., Kogure,K., Akita,H. and Harashima,H. (2006) Uptake pathways and subsequent intracellular trafficking in nonviral gene delivery. *Pharmacol. Rev.*, **58**, 32–45.
31. Al Soraj,M., He,L., Peynshaert,K., Cousaert,J., Vercauteren,D., Braeckmans,K., De Smedt,S.C. and Jones,A.T. (2012) siRNA and pharmacological inhibition of endocytic pathways to characterize the differential role of macropinocytosis and the actin cytoskeleton on cellular uptake of dextran and cationic cell penetrating peptides octaarginine (R8) and HIV-Tat. *J. Control Release.*, **161**, 132–141.
32. Akinc,A., Querbes,W., De,S., Qin,J., Frank-Kamenetsky,M., Jayaprakash,K.N., Jayaraman,M., Rajeev,K.G., Cantley,W.L., Dorkin,J.R. *et al.* (2010) Targeted delivery of RNAi therapeutics with endogenous and exogenous ligand-based mechanisms. *Mol. Ther.*, **18**, 1357–1364.
33. Ming,X., Sato,K. and Juliano,R.L. (2011) Unconventional internalization mechanisms underlying functional delivery of antisense oligonucleotides via cationic lipoplexes and polyplexes. *J. Control Release*, **153**, 83–92.
34. Detzer,A. and Sczakiel,G. (2009) Phosphorothioate-stimulated uptake of siRNA by mammalian cells: a novel route for delivery. *Curr. Top. Med. Chem.*, **9**, 1109–1116.
35. Alam,M.R., Dixit,V., Kang,H., Li,Z.B., Chen,X., Trejo,J., Fisher,M. and Juliano,R.L. (2008) Intracellular delivery of an anionic antisense oligonucleotide via receptor-mediated endocytosis. *Nucleic Acids Res.*, **36**, 2764–2776.
36. Alam,M.R., Ming,X., Dixit,V., Fisher,M., Chen,X. and Juliano,R.L. (2010) The biological effect of an antisense oligonucleotide depends on its route of endocytosis and trafficking. *Oligonucleotides*, **20**, 103–109.
37. Koller,E., Vincent,T.M., Chappell,A., De,S., Manoharan,M. and Bennett,C.F. (2011) Mechanisms of single-stranded phosphorothioate modified antisense oligonucleotide accumulation in hepatocytes. *Nucleic Acids Res.*, **39**, 4795–4807.
38. Kortylewski,M., Swiderski,P., Herrmann,A., Wang,L., Kowolik,C., Kujawski,M., Lee,H., Scuto,A., Liu,Y., Yang,C. *et al.* (2009) In vivo delivery of siRNA to immune cells by conjugation to a TLR9 agonist enhances antitumor immune responses. *Nat. Biotechnol.*, **27**, 925–932.
39. Ming,X., Alam,M.R., Fisher,M., Yan,Y., Chen,X. and Juliano,R.L. (2010) Intracellular delivery of an antisense oligonucleotide via endocytosis of a G protein-coupled receptor. *Nucleic Acids Res.*, **38**, 6567–6576.
40. Hutagalung,A.H. and Novick,P.J. (2011) Role of Rab GTPases in membrane traffic and cell physiology. *Physiol. Rev.*, **91**, 119–149.
41. Stechmann,B., Bai,S.K., Gobbo,E., Lopez,R., Merer,G., Pinchard,S., Panigai,L., Tenza,D., Raposo,G., Beaumelle,B. *et al.* (2010) Inhibition of retrograde transport protects mice from lethal ricin challenge. *Cell*, **141**, 231–242.
42. Johannes,L. and Popoff,V. (2008) Tracing the retrograde route in protein trafficking. *Cell*, **135**, 1175–1187.
43. Alahari,S.K., Dean,N.M., Fisher,M.H., Delong,R., Manoharan,M., Tivel,K.L. and Juliano,R.L. (1996) Inhibition of expression of the multidrug resistance-associated P-glycoprotein of by phosphorothioate and 5' cholesterol-conjugated phosphorothioate antisense oligonucleotides. *Mol. Pharmacol.*, **50**, 808–819.
44. Taylor,J.K., Zhang,Q.Q., Monia,B.P., Marcusson,E.G. and Dean,N.M. (1999) Inhibition of Bcl-xL expression sensitizes normal human keratinocytes and epithelial cells to apoptotic stimuli. *Oncogene*, **18**, 4495–4504.
45. Xu,D., Kang,H., Fisher,M. and Juliano,R.L. (2004) Strategies for inhibition of MDR1 gene expression. *Mol. Pharmacol.*, **66**, 268–275.
46. Bauman,J.A., Li,S.D., Yang,A., Huang,L. and Kole,R. (2010) Anti-tumor activity of splice-switching oligonucleotides. *Nucleic Acids Res.*, **38**, 8348–8356.
47. Fisher,M., Abramov,M., Van Aerschot,A., Xu,D., Juliano,R.L. and Herdewijn,P. (2007) Inhibition of MDR1 expression with altritol-modified siRNAs. *Nucleic Acids Res.*, **35**, 1064–1074.
48. Eytan,G.D., Regev,R., Oren,G., Hurwitz,C.D. and Assaraf,Y.G. (1997) Efficiency of P-glycoprotein-mediated exclusion of rhodamine dyes from multidrug-resistant cells is determined by

their passive transmembrane movement rate. *Eur. J. Biochem.*, **248**, 104–112.
49. Ming,X., Ju,W., Wu,H., Tidwell,R.R., Hall,J.E. and Thakker,D.R. (2009) Transport of dicationic drugs pentamidine and furamidine by human organic cation transporters. *Drug Metab. Dispos.*, **37**, 424–430.
50. Dunn,K.W., Kamocka,M.M. and McDonald,J.H. (2011) A practical guide to evaluating colocalization in biological microscopy. *Am. J. Physiol. Cell Physiol.*, **300**, C723–C742.
51. Rice,B.W., Cable,M.D. and Nelson,M.B. (2001) In vivo imaging of light-emitting probes. *J. Biomed. Opt.*, **6**, 432–440.
52. Ambudkar,S.V., Kimchi-Sarfaty,C., Sauna,Z.E. and Gottesman,M.M. (2003) P-glycoprotein: from genomics to mechanism. *Oncogene*, **22**, 7468–7485.
53. Lipinski,C.A., Lombardo,F., Dominy,B.W. and Feeney,P.J. (2001) Experimental and computational approaches to estimate solubility and permeability in drug discovery and development settings. *Adv. Drug Deliv. Rev.*, **46**, 3–26.
54. Decker,T. and Lohmann-Matthes,M.L. (1988) A quick and simple method for the quantitation of lactate dehydrogenase release in measurements of cellular cytotoxicity and tumor necrosis factor (TNF) activity. *J. Immunol. Methods*, **115**, 61–69.
55. Turner,J.J., Ivanova,G.D., Verbeure,B., Williams,D., Arzumanov,A.A., Abes,S., Lebleu,B. and Gait,M.J. (2005) Cell-penetrating peptide conjugates of peptide nucleic acids (PNA) as inhibitors of HIV-1 Tat-dependent trans-activation in cells. *Nucleic Acids Res.*, **33**, 6837–6849.
56. Chin,D.J., Green,G.A., Zon,G., Szoka,F.C. Jr and Straubinger,R.M. (1990) Rapid nuclear accumulation of injected oligodeoxyribonucleotides. *New Biol.*, **2**, 1091–1100.
57. Stenmark,H. (2009) Rab GTPases as coordinators of vesicle traffic. *Nat. Rev. Mol. Cell Biol.*, **10**, 513–525.
58. Storrie,B., White,J., Rottger,S., Stelzer,E.H., Suganuma,T. and Nilsson,T. (1998) Recycling of golgi-resident glycosyltransferases through the ER reveals a novel pathway and provides an explanation for nocodazole-induced Golgi scattering. *J. Cell Biol.*, **143**, 1505–1521.
59. Howe,C.L., Granger,B.L., Hull,M., Green,S.A., Gabel,C.A., Helenius,A. and Mellman,I. (1988) Derived protein sequence, oligosaccharides, and membrane insertion of the 120-kDa lysosomal membrane glycoprotein (lgp120): identification of a highly conserved family of lysosomal membrane glycoproteins. *Proc. Natl Acad. Sci. USA*, **85**, 7577–7581.
60. Wolf,Y., Pritz,S., Abes,S., Bienert,M., Lebleu,B. and Oehlke,J. (2006) Structural requirements for cellular uptake and antisense activity of peptide nucleic acids conjugated with various peptides. *Biochemistry*, **45**, 14944–14954.
61. Midoux,P., Pichon,C., Yaouanc,J.J. and Jaffres,P.A. (2009) Chemical vectors for gene delivery: a current review on polymers, peptides and lipids containing histidine or imidazole as nucleic acids carriers. *Br. J. Pharmacol.*, **157**, 166–178.
62. Ivanova,G.D., Arzumanov,A., Abes,R., Yin,H., Wood,M.J., Lebleu,B. and Gait,M.J. (2008) Improved cell-penetrating peptide-PNA conjugates for splicing redirection in HeLa cells and exon skipping in mdx mouse muscle. *Nucleic Acids Res.*, **36**, 6418–6428.
63. Yamamoto,T., Nakatani,M., Narukawa,K. and Obika,S. (2011) Antisense drug discovery and development. *Future Med. Chem.*, **3**, 339–365.
64. Nielsen,P.E. (2010) Gene targeting and expression modulation by peptide nucleic acids (PNA). *Curr. Pharm. Des.*, **16**, 3118–3123.
65. Lima,W.F., Prakash,T.P., Murray,H.M., Kinberger,G.A., Li,W., Chappell,A.E., Li,C.S., Murray,S.F., Gaus,H., Seth,P.P. *et al.* (2012) Single-stranded siRNAs activate RNAi in animals. *Cell*, **150**, 883–894.
66. Juliano,R.L., Ming,X. and Nakagawa,O. (2012) The chemistry and biology of oligonucleotide conjugates. *Acc. Chem. Res.*, **45**, 1067–1076.
67. Wheeler,L.A., Trifonova,R., Vrbanac,V., Basar,E., McKernan,S., Xu,Z., Seung,E., Deruaz,M., Dudek,T., Einarsson,J.I. *et al.* (2011) Inhibition of HIV transmission in human cervicovaginal explants and humanized mice using CD4 aptamer-siRNA chimeras. *J. Clin. Invest.*, **121**, 2401–2412.
68. Zammarchi,F., de Stanchina,E., Bournazou,E., Supakorndej,T., Martires,K., Riedel,E., Corben,A.D., Bromberg,J.F. and Cartegni,L. (2011) Antitumorigenic potential of STAT3 alternative splicing modulation. *Proc. Natl Acad. Sci. USA*, **108**, 17779–17784.
69. Young,D.D., Connelly,C.M., Grohmann,C. and Deiters,A. (2010) Small molecule modifiers of microRNA miR-122 function for the treatment of hepatitis C virus infection and hepatocellular carcinoma. *J. Am. Chem. Soc.*, **132**, 7976–7981.
70. Tan,G.S., Chiu,C.H., Garchow,B.G., Metzler,D., Diamond,S.L. and Kiriakidou,M. (2012) Small molecule inhibition of RISC loading. *ACS Chem. Biol.*, **7**, 403–410.
71. Giorgianna,W.Y. and Young,D.D. (2011) Development and utilization of non-coding RNA-small molecule interactions. *Org. Biomol. Chem.*, **9**, 7969–7978.
72. Kendall,G.C., Mokhonova,E.I., Moran,M., Sejbuk,N.E., Wang,D.W., Silva,O., Wang,R.T., Martinez,L., Lu,Q.L., Damoiseaux,R. *et al.* (2012) Dantrolene enhances antisense-mediated exon skipping in human and mouse models of duchenne muscular dystrophy. *Sci. Transl. Med.*, **4**, 164ra160.